J. Fluid Mech. (2002), *vol.* 466, *pp.* 205–214.
DOI: 10.1017/S0022112002001313 Printed in the United Kingdom

Horizontal convection is non-turbulent

By F. PAPARELLA[1] AND W. R. YOUNG[2]

[1]Department of Mathematics, University of Lecce, Italy

[2]Scripps Institution of Oceanography, La Jolla, CA 92093-0213, USA

(Received 27 April 2002 and in revised form 22 May 2002)

Consider the problem of horizontal convection: a Boussinesq fluid, forced by applying a non-uniform temperature at its top surface, with all other boundaries insulating. We prove that if the viscosity, ν, and thermal diffusivity, κ, are lowered to zero, with $\sigma \equiv \nu/\kappa$ fixed, then the energy dissipation per unit mass, ε, also vanishes in this limit. Numerical solutions of the two-dimensional case show that despite this anti-turbulence theorem, horizontal convection exhibits a transition to eddying flow, provided that the Rayleigh number is sufficiently high, or the Prandtl number σ sufficiently small. We speculate that horizontal convection is an example of a flow with a large number of active modes which is nonetheless not 'truly turbulent' because $\varepsilon \to 0$ in the inviscid limit.

1. Introduction

A key feature of the ocean and the stratosphere is that the solar irradiance forces the fluid differentially in latitude and sets up strongly stable density stratification. This situation is very different from the Rayleigh–Bénard paradigm, in which a fluid is heated from below and cooled at the top. A more appropriate geophysical idealization, suggested by Stommel (1962), is the experiment of Rossby (1965) illustrated in figure 1. We follow Stern (1975) in referring to this flow configuration as 'horizontal convection'.

Because the surface temperature is uneven, there are horizontal density and pressure gradients and the fluid is in motion. Indeed, the critical Rayleigh number for the onset of horizontal convection is zero: the smallest ΔT sets the fluid into motion. But in the geophysical situation the Rayleigh and Reynolds numbers (denoted generically by R) are enormous. In many situations, this statement is the prelude to a discussion of turbulent flow. Yet we show below that Rossby's experiment cannot become 'truly turbulent', even if $R \to \infty$. By 'true turbulence' we do not mean merely sensitive dependence on initial conditions, or even the dynamics of many coupled modes. We mean that the two experimental laws of fully developed turbulence apply (Frisch 1995). The first law requires a spectral cascade, as envisaged by Richardson. Our main focus is however:

The law of finite energy dissipation: If, in an experiment on turbulent flow, all the control parameters are kept the same, except for the viscosity, ν, which is lowered as much as possible, the energy dissipation per unit mass behaves in a way consistent with a finite positive limit.

The main implication of the law of finite energy dissipation is that the energy dissipation per unit mass, Kolmogorov's ε, is non-zero in the inviscid limit $R \to \infty$.

The law of finite energy dissipation is also known as the 'zeroth' law of turbulence. Experimental evidence in support of it is provided by measurements of ε in

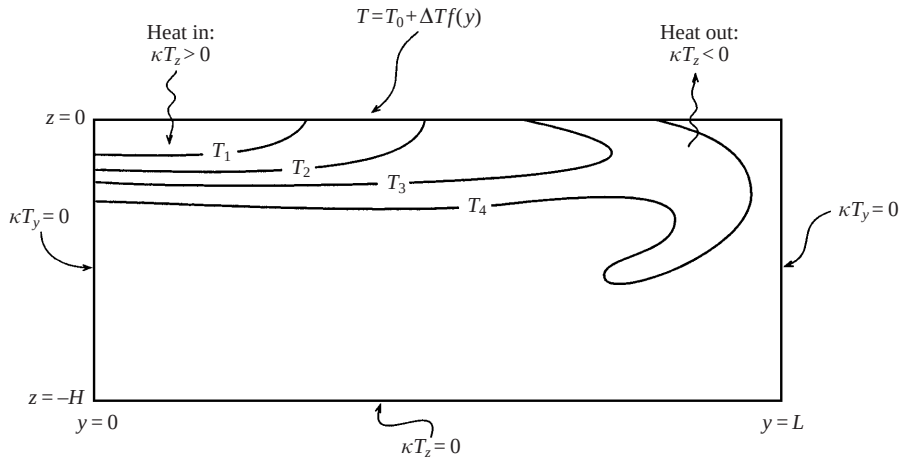

FIGURE 1. A schematic illustration of horizontal convection. There is a small region of statically unstable fluid indicated in the upper right corner, where heat is leaving the box. But over most of the volume the stratification is stable, i.e. $T_z > 0$. The Rayleigh number is $R \equiv g\alpha\Delta T H^3/\nu\kappa$. As an indication of the oceanographic parameter range take the depth of the layer as $H = 1\,\mathrm{km}$, $\kappa = 10^{-7}\,\mathrm{m^2\,s^{-1}}$, $\nu = 10\kappa$, and $g' \equiv g\alpha\Delta T = 10^{-2}\,\mathrm{m^2\,s^{-1}}$. Then $R = 10^{20}$. The geophysical aspect ratio is $L/H \sim 1000$ and for water $\sigma \equiv \nu/\kappa \sim 10$.

grid-generated turbulence (Sreenivasan 1984). And Sreenivasan (1998) summarizes the results of numerical simulations of homogeneous turbulence showing that ε is independent of viscosity at large Reynolds number. On the other hand, experiments by Cadot *et al.* (1997) – with Reynolds numbers of order 10^6 – show that the law is violated for Taylor–Couette flow and in a flow driven by smooth counter-rotating disks.

For horizontal convection the salient theoretical result, which we prove below, is:

The anti-turbulence theorem: If the only forcing is non-uniform heating applied at the surface of a Boussinesq fluid and if the viscosity, ν, and thermal diffusivity, κ, are lowered to zero, with $\sigma \equiv \nu/\kappa$ fixed, then the energy dissipation ε also vanishes.

The anti-turbulence theorem makes rigorous an earlier argument that surface heating alone is not an effective mechanism for supplying energy to the ocean circulation (Sandström 1908; Defant 1961; Houghton 1986). This result, often referred to as 'Sandström's Theorem', is based on thermodynamics and was not derived from the fluid equations. In fact, as pointed out by Jeffreys (1925), Sandström's argument is flawed because it does not account for the molecular diffusion of heat. With the anti-turbulence theorem, we see exactly in what light one can view Sandström's result as rigorous.

Munk & Wunsch (1998) used Sandström's argument as a springboard for a discussion of the energy balance of oceanic turbulence. Munk & Wunsch argue that the planetary-scale ocean circulation, estimated to provide an equator-to-pole heat flux of $2 \times 10^{15}\,\mathrm{W}$, is an incidental or passive consequence of a circulation which is really driven by $2 \times 10^{12}\,\mathrm{W}$ of wind and tidal forcing. The anti-turbulence theorem supports this conclusion: a hypothetical ocean circulation, driven only by surface heating, could not exhibit the observed small-scale marine turbulence. Instead, the wind and the tides must be the sources of turbulent power which enables the ocean circulation to transport heat. In other words, the ocean circulation is *not* driven by the difference in density between equator and pole; rather the circulation is a heat and salt conveyor belt powered by wind and tides.

2. Formulation

We consider a three-dimensional rotating fluid (Coriolis frequency f) in a rectangular box. The vertical coordinate is $-H < z < 0$. At the top, $z = 0$, some pattern of non-uniform heating and cooling is imposed by external forcing. There is no flux of heat through the bottom, $z = -H$, or through the sidewalls. We use the Boussinesq approximation and represent the density as $\rho = \rho_0(1-g^{-1}b)$ where b is the 'buoyancy'. In more familiar notation $b = g\alpha(T - T_0)$, where T is the temperature of the fluid and T_0 is a constant reference temperature. The Boussinesq equations of motion are

$$\left.\begin{aligned} \frac{\mathrm{D}\boldsymbol{u}}{\mathrm{D}t} + \hat{\boldsymbol{z}} \times f\boldsymbol{u} + \nabla p = b\hat{\boldsymbol{z}} + \nu\nabla^2\boldsymbol{u}, \\ \frac{\mathrm{D}b}{\mathrm{D}t} = \kappa\nabla^2 b, \\ \nabla \cdot \boldsymbol{u} = 0. \end{aligned}\right\} \tag{2.1}$$

The boundary conditions on the velocity $\boldsymbol{u} = (u, v, w)$ are $\boldsymbol{u} \cdot \hat{\boldsymbol{n}} = 0$, where $\hat{\boldsymbol{n}}$ is the outward normal, and some combination of no slip and no stress. We specify the buoyancy on the top; an illustrative example used below is

$$b(x, y, 0, t) = b_{\max} \sin^2(\pi y/L), \tag{2.2}$$

with $-L/2 < y < L/2$.

We use an overbar to denote the horizontal average over x and y. If the solution is unsteady we also include a time average in the overbar. In any event, we assume that with sufficient time and space averaging, all overbarred fields are steady. Thus $\bar{b}$ is a function only of z. It follows from (2.1), and from the no-flux condition at $z = -H$, that

$$\overline{wb} - \kappa\bar{b}_z = 0. \tag{2.3}$$

Thus there is no net vertical buoyancy flux through every level $z =$ constant.

To measure the strength of horizontal convection we must define a suitable non-dimensional measure. The familiar Nusselt number of the Rayleigh–Bénard problem is not useful because from (2.3) the heat flux is zero. Instead we construct an alternative index of the intensity of convection by first solving the conduction problem

$$\nabla^2 c = 0, \tag{2.4}$$

using the same boundary conditions on c as on b. Then we define the non-dimensional functional

$$\Phi[b] \equiv \frac{\int \nabla b \cdot \nabla b \, \mathrm{d}V}{\int \nabla c \cdot \nabla c \, \mathrm{d}V}, \tag{2.5}$$

where the integral is over the volume of the box. In physical terms Φ is the ratio of entropy production in the convecting flow to the entropy production of the conductive solution. One can show using a standard argument that Φ is always greater than unity. In the numerical simulations of § 4 we use Φ as a global measure of the strength of horizontal convection.

3. The anti-turbulence theorem

We denote the average over the volume of the box by angular brackets:

$$\langle\theta\rangle \equiv V^{-1}\int \theta(x,y,z,t)\,\mathrm{d}V = H^{-1}\int_{-H}^{0}\bar{\theta}(z)\,\mathrm{d}z. \tag{3.1}$$

Taking the dot product of the momentum equation in (2.1) with $\boldsymbol{u}$ and averaging over the volume, one has

$$\varepsilon \equiv \nu\langle\|\boldsymbol{\nabla u}\|^2\rangle = \langle wb\rangle, \tag{3.2}$$

where $\|\boldsymbol{\nabla u}\|^2 \equiv \nabla u\cdot\nabla u + \nabla v\cdot\nabla v + \nabla w\cdot\nabla w$ is the deformation, and ε is the mechanical energy dissipation per unit mass; (3.2) shows that ε is supplied by the conversion of potential energy into kinetic energy via the correlation in $\langle wb\rangle$.

Another expression for the buoyancy flux $\langle wb\rangle$ is obtained by averaging (2.3) over z:

$$\langle wb\rangle = \kappa H^{-1}[\bar{b}(0) - \bar{b}(-H)]. \tag{3.3}$$

Eliminating the buoyancy flux $\langle wb\rangle$ between the kinetic energy integral (3.2) and the potential energy integral (3.3) one then has

$$\nu\langle\|\boldsymbol{\nabla u}\|^2\rangle = \kappa H^{-1}[\bar{b}(0) - \bar{b}(-H)]. \tag{3.4}$$

The source on the right-hand side of (3.4) is bounded because the buoyancy in the box must lie between the maximum and minimum values imposed at the surface (e.g. Protter & Weinberger 1984):

$$\bar{b}(0) - \bar{b}(-H) < b_{\max}. \tag{3.5}$$

(As in (2.2), we suppose for convenience that $b_{\min} = 0$.) Using inequality (3.5), equation (3.4) implies that

$$\varepsilon \equiv \nu\langle\|\boldsymbol{\nabla u}\|^2\rangle < \kappa H^{-1} b_{\max}. \tag{3.6}$$

Taking a limit $\kappa \to 0$ (with $b_{\max}$ and H fixed) one concludes from (3.6) that $\varepsilon \to 0$. In particular, one also reaches this conclusion by taking the fixed-σ limit in which all external parameters are fixed except that $(\nu,\kappa) \to 0$ with $\sigma \equiv \nu/\kappa$ constant. This anti-turbulence theorem provides a rigorous foundation for both Sandström's (1908) thermodynamic argument and its recent applications in geophysics.

4. Numerical solutions

It follows from the zero-flux condition (2.3) that at $z = 0$, where $w = 0$, we have $\bar{b}_z(0) = 0$. Consequently the vertical buoyancy gradient at the top, $b_z(x,y,0,t)$, must have both signs. This implies that the fluid is statically unstable (that is $b_z < 0$) beneath the point at which the surface buoyancy is a minimum. At this location there is a plume which continuously fills the abyss with dense fluid. To balance the downwards mass flux in the plume there is a large-scale upwelling which lifts the deep dense fluid back to the surface. This flow towards the surface ensures that the imposed non-uniform surface temperature penetrates diffusively only a small distance into the fluid. In the limiting case $\sigma = \infty$, Rossby (1965) gives a scaling argument for the thickness of this thermal boundary layer.

The numerical simulations of horizontal convection reported by Somerville (1967), Beardsley & Festa (1972) and Rossby (1998) are consistent with the scenario described above and further indicate that the flow is steady (e.g. the plume is laminar). Based on these numerical results, and on Sandström's argument, it has been concluded

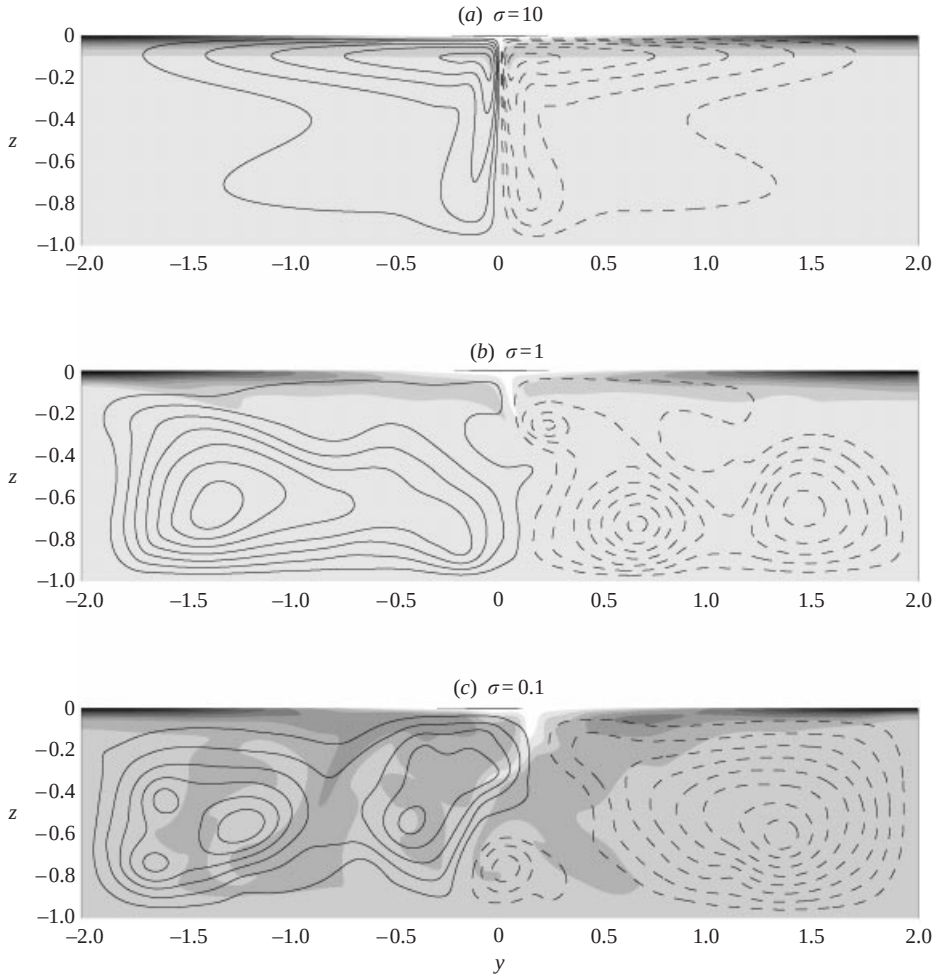

FIGURE 2. Numerical solutions of the two-dimensional Rossby problem obtained using the surface temperature distribution (2.2); the plume is in the middle of the domain at $y = 0$, and $R = 10^8$. The solid lines indicate the streamfunction and the shading shows the buoyancy (equivalently temperature). Panel (a) shows a steady, stable circulation with Prandtl number $\sigma = 10$ (close to that of water). Panels (b, c) show that a transition to unsteady flow occurs as σ is decreased at fixed Rayleigh number, $R \equiv b_{\max} H^3/\nu\kappa$.

that horizontal convection must be steady and stable even as $R \to \infty$ (e.g. Huang 1999; Wunsch 2000). This conclusion is also drawn in a recent textbook (chapter 1 of Houghton 1986), and considered as a relevant factor in determining the thermal structure of the atmosphere of Venus.

Nevertheless, the conclusion that the flow is steady and stable as $R \to \infty$ is a far stronger claim than can be expected from the anti-turbulence theorem. This result states only that uneven surface heating cannot provide net energy to the fluid in the inviscid limit. The gap between the steady assumption and the anti-turbulence theorem led us to undertake a suite of numerical simulations of the two-dimensional, non-rotating ($f = 0$) version of Rossby's problem.

We used the surface forcing function in (2.2) and solved the equations of motion using the vorticity–streamfunction formulation with stress-free boundary conditions.

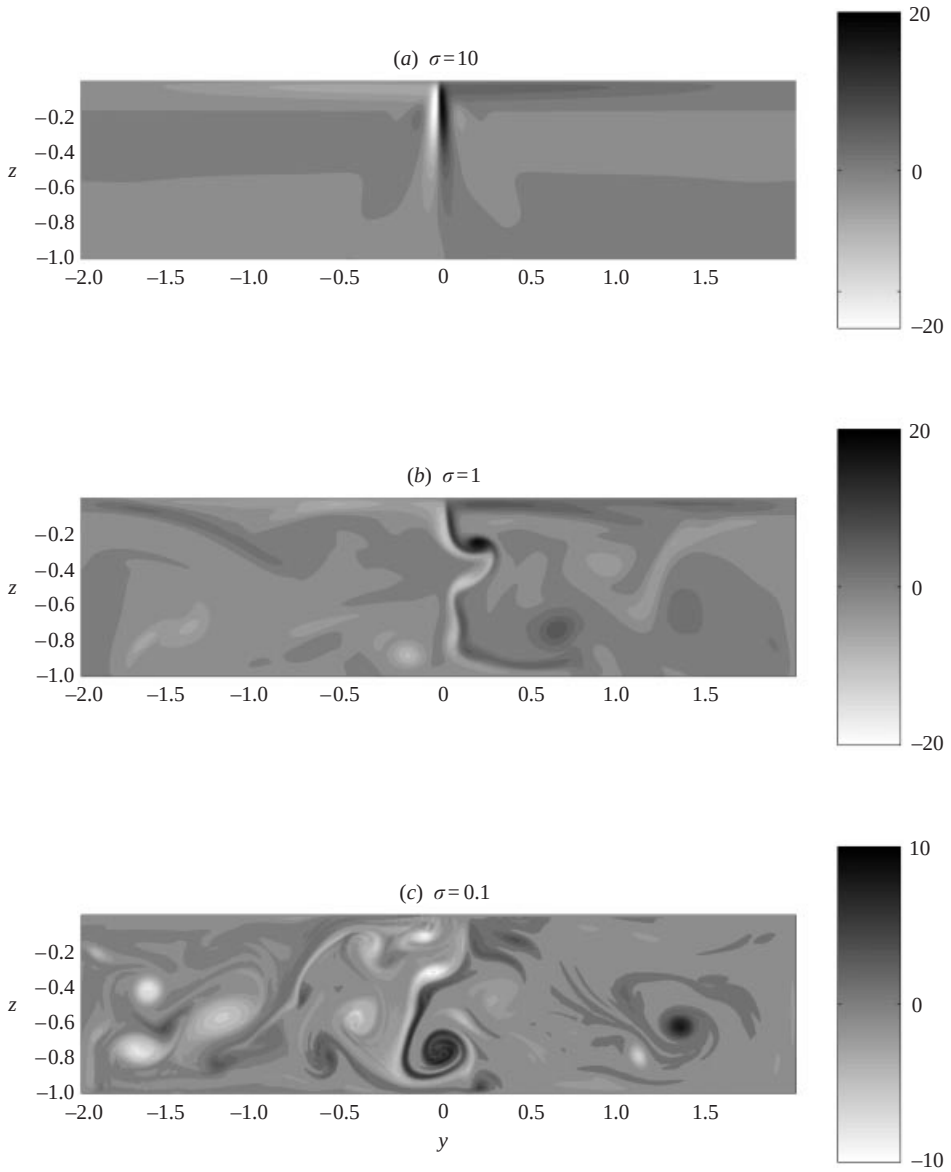

FIGURE 3. To solve the two-dimensional problem we use the streamfunction (ψ)-vorticity ($\nabla^2\psi$) formulation for $R = 10^8$. The panels above show the vorticity, $\nabla^2\psi$, corresponding to figure 2(a–c). Panel (c) shows the vortices generated by the instability of the plume.

The calculations are characterized by three non-dimensional parameters: the Rayleigh number $R \equiv b_{\max}H^3/\nu\kappa$; the Prandtl number $\sigma \equiv \nu/\kappa$; the aspect ratio H/L. All simulations start from rest with a constant buoyancy (typically $b(x, z, 0) = 0.5b_{\max}$), and run till $\kappa t/H^2 = 20$. The resolution is 128×32 grid points for $R = 10^6$ or less, and increases to 512×128 grid points for $R = 10^8$. The numerical code solves the prognostic equations for buoyancy and vorticity on a staggered grid with a second-order discretization, both in space and time. The elliptic problem for the streamfunction is solved with a multigrid method.

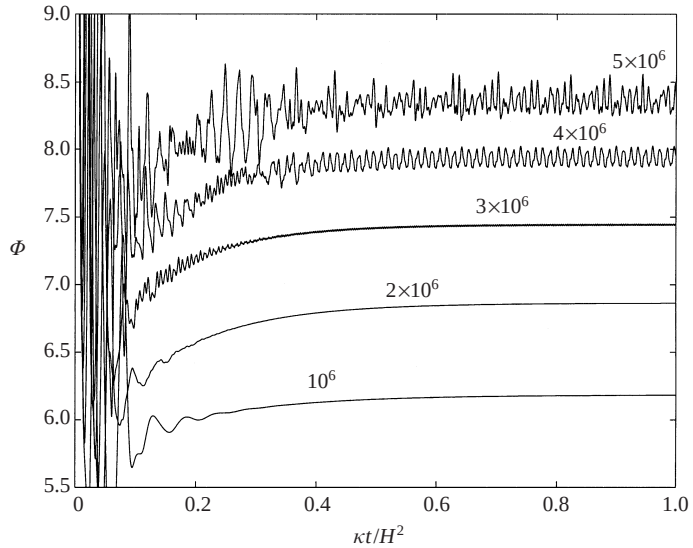

FIGURE 4. A suite of calculations at $\sigma = 1$; the curves are labelled by the Rayleigh number R. The non-dimensional functional Φ is defined in (2.5) and the surface forcing function is defined in (2.2). The run at $R = 3 \times 10^6$ is weakly unsteady as evidenced by a slight thickening of the curve.

The numerical results are at odds with the steady-flow scenario: the steady flow set up by the surface forcing becomes unstable and evolves unsteadily at sufficiently high Rayleigh numbers – see figures 2 and 3. The threshold for the transition depends on both Rayleigh and Prandtl numbers: figures 2(*a*) and 3(*a*) show a steady and stable flow which is similar to the results of Rossby (1998). But figures 2(*b*,*c*) and 3(*b*,*c*) show that this flow becomes unsteady as the Prandtl number, $\sigma \equiv \nu/\kappa$, is decreased holding the Rayleigh number, R, fixed. A sequence of computations, varying R with $(\sigma, H/L) = (1, 1/4)$, is shown in figure 4. These computations indicate that the transition to unsteady flow occurs at $R \approx 3 \times 10^6$. Figure 5 summarizes a suite of calculations in which we located this transition in the (R, σ) parameter plane.

Eddying flow has not been previously observed presumably because the earlier numerical studies did not penetrate into the unstable portion of the $(\sigma, L/H, R)$ parameter space. The calculations reported here differ from earlier investigations because: (i) we use higher Rayleigh numbers and smaller Prandtl numbers; (ii) the aspect ratio is $L/H = 4$ in our case, and $L/H = 1$ in that of Rossby (1998); (iii) our surface boundary condition in (2.2) moves the plume away from a sidewall and into the middle of the container. Modifications (ii) and (iii) may lead to a destabilization of the flow at lower Rayleigh numbers. We speculate that a transition to unsteady flow will occur even in Rossby's $\sigma = 10$ configuration provided that the Rayleigh number can be increased sufficiently.

The anti-turbulence theorem in § 3 applies to the full three-dimensional Boussinesq equations. On the other hand, the calculations in this section are of the two-dimensional problem. These two-dimensional solutions are sufficient to refute the view that horizontal convection is always steady and stable. Indeed, we expect that the transition to eddying flow will occur at significantly lower Rayleigh numbers (and probably via a different instability) in the three-dimensional case.

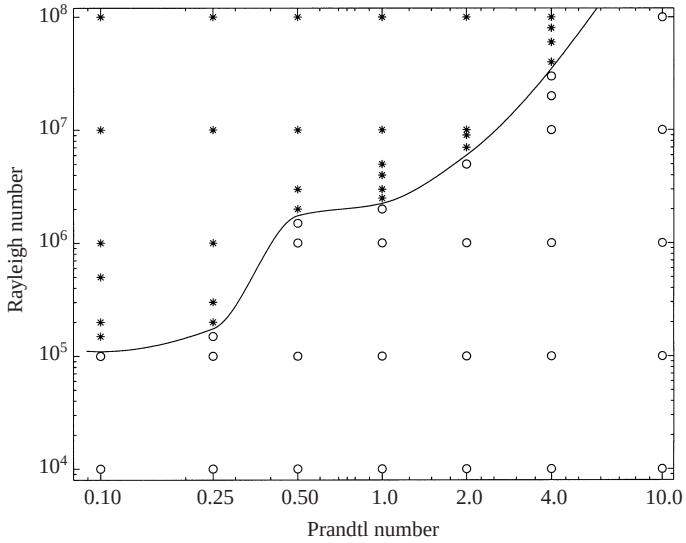

FIGURE 5. The boundary between steady and unsteady solutions in the (R, σ)-plane. In all cases $L/H = 4$ and the surface forcing function is defined in (2.2). The open circles indicate steady solutions and the stars unsteady solutions. This stability boundary is for the two-dimensional system: the three-dimensional system will transition at smaller Rayleigh number.

5. Conclusions and discussion

It is interesting to compare horizontal convection with the classical Rayleigh–Bénard (RB) problem. For instance, does RB convection satisfy the law of finite energy dissipation? Our arguments use the crucial result (2.3): in horizontal convection the net vertical buoyancy flux is zero. But in the RB case the buoyancy flux is a non-zero constant and this non-zero flux produces an additional contribution to the RB analogue of the energy power integral in (3.4). For this reason clear-cut conclusions concerning the inviscid limit of ε for the RB system cannot be reached using the energy power integral alone. Instead, more elaborate variational arguments are called for (e.g. Howard 1963; Busse 1969).

In astrophysics and geophysics an ultimate RB regime in which the vertical transport of heat is independent of the molecular parameters ν and κ is often invoked in mixing-length theories of turbulent transport. In terms of non-dimensional variables, the molecular parameters are irrelevant if and only if the RB Nusselt number scales as $R^{1/2}$ (Kraichnan 1962; Spiegel 1971; Siggia 1994). Any power-law scaling for the RB Nusselt number with an exponent less than the ultimate exponent, $1/2$, implies not only that ν and κ are relevant for heat transport but also that the flow is non-turbulent flow according to the criterion we have used in this work.

There are no laboratory experiments or numerical simulations which unambiguously show that RB heat flux becomes independent of molecular parameters as $R \to \infty$. Indeed, Niemela *et al.* (2000) show that heat transport depends on the molecular parameters for Rayleigh numbers as large as 10^{17}. Thus the most recent experimental evidence indicates that RB convection also violates the law of finite energy dissipation.

There may also be other flows in which the law of finite energy dissipation is weakly violated. Recent estimates suggest that ε might decay as some inverse power of $\ln R$ for wall-bounded shear flows and convection. For example, Doering, Spiegel

& Worthing (2000) indicate that turbulent shear flows with smooth walls might have $\varepsilon \sim 1/(\ln R)^2$ as $R \to \infty$ (see also Cadot *et al.* 1997). Logarithmically weak dependence on R is difficult to detect experimentally and perhaps there are other 'turbulent' flows in which ε vanishes slowly as R is increased. If such examples are common then the definition of turbulent motion as demanding non-zero ε is too strict. In any event, horizontal convection holds a special place amongst these examples because only in this case do power integrals produce a constraint as forceful as (3.6).

This work was supported by the National Science Foundation under the "Collaborations in Mathematical Geophysics" program, and partly carried out at the 1999 Geophysical Fluid Dynamics (GFD) Program hosted by the Woods Hole Oceanographic Institution. We thank Neil Balmforth, Paola Cessi, Charlie Doering, Giorgio Metafune, Ed Spiegel and Carl Wunsch for helpful discussion of this problem. We also thank the anonymous referees whose comments improved this work. The GFD program is supported by the National Science Foundation and the Office of Naval Research.

REFERENCES

Beardsley, R. C. & Festa, J. F. 1972 A numerical model of convection driven by a surface stress and non-uniform horizontal heating. *J. Phys. Oceanogr.* **2**, 444–455.

Busse, F. H. 1969 On Howard's bound for heat transport by turbulent convection. *J. Fluid Mech.* **37**, 457–477.

Cadot, O., Couder, Y., Daerr, A., Douady, S. & Tsinober, A. 1997 Energy injection in a closed turbulent flow: stirring through boundary layers versus inertial stirring. *Phys. Rev.* E **56**, 427.

Defant, A. 1961 *Physical Oceanography*, Vol. I. MacMillan.

Doering, C. R., Spiegel, E. A. & Worthing, R. A. 2000 Energy dissipation in a shear layer with suction. *Phys. Fluids* **12**, 1955–1968.

Frisch, U. 1995 *Turbulence: the Legacy of A. N. Kolmogorov*. Cambridge University Press.

Houghton, J. T. 1986 *The Physics of Atmospheres*, 2nd Edn. Cambridge University Press.

Howard, L. N. 1963 Heat transport by turbulent convection. *J. Fluid Mech.* **17**, 405–432.

Huang, R. X. 1999 Mixing and energetics of the oceanic thermohaline circulation. *J. Phys. Oceanogr.* **29**, 727–746.

Jeffreys, H. 1925 On fluid motions produced by differences of temperature and humidity. *Q. J. R. Met. Soc.* **51**, 347–356.

Kraichnan, R. H. 1962 Turbulent thermal convection at arbitrary Prandtl number. *Phys. Fluids* **5**, 1374–1389.

Munk, W. H. & Wunsch, C. 1998 Abyssal recipes II: energetics of tidal and wind mixing. *Deep-Sea Res.* **45**, 1977–2010.

Niemela, J. J., Skrbek, L., Sreenivasan, K. R. & Donnelly, R. J. 2000 Turbulent convection at very high Rayleigh numbers. *Nature* **404**, 837–841.

Protter, M. H. & Weinberger, H. F. 1984 *Maximum Principles in Differential Equations*. Springer.

Rossby, T. 1965 On thermal convection driven by non-uniform heating from below: an experimental study. *Deep-Sea Res.* **12**, 9–16.

Rossby, T. 1998 Numerical experiments with a fluid heated non-uniformly from below. *Tellus* **50A**, 242–257.

Sandström, J. W. 1908 Dynamische Versuche mit Meerwasser. *Annals in Hydrodynamic Marine Meteorology*.

Siggia, E. D. 1994 High Rayleigh number convection. *Annu. Rev. Fluid Mech.* **26**, 137–168.

Somerville, R. C. 1967 A non-linear spectral model of convection in a fluid unevenly heated from below. *J. Atmos. Sci.* **24**, 665–676.

Spiegel, E. A. 1971 Convection in stars. *Annu. Rev. Astron. Astrophys.* **9**, 323–352.

Sreenivasan, K. R. 1984 On the scaling of turbulence energy dissipation rate. *Phys. Fluids* **27**, 1048–1051.

Sreenivasan, K. R. 1998 An update on the dissipation rate in homogeneous turbulence. *Phys. Fluids* **10**, 528–529.

Stommel, H. 1962 On the smallness of the sinking regions in the ocean. *Proc. Natl Acad. Sci.* **48**, 766–772.

Stern, M. E. 1975 *Ocean Circulation Physics*. Academic.

Wunsch, C. 2000 Moon, tides and climate. *Nature* **405**, 743–744.